



Cite this: *Dalton Trans.*, 2015, **44**, 9659

Fluorescent benzene-centered mono-, bis- and tris-triazapentadiene–boron complexes†‡

Christoph Glotzbach,^a Nadine Gödeke,^a Roland Fröhlich,^a Constantin-Gabriel Daniliuc,^a Shohei Saito,^b Shigehiro Yamaguchi^b and Ernst-Ulrich Würthwein^{*a}

A series of novel benzene centered mono-, bis- and tris-1,3,5-triazapentadiene ligands **6a–e** was synthesized and investigated with respect to their reactivity towards triphenylborane. The resulting blue-fluorescent boron complexes **14a–e** with a six-membered ring chelate structure show excellent thermal and chemical stability. All title compounds were completely characterized including X-ray diffraction studies for **14a–c** and **14e**. Whereas the absorption spectra of all three classes of compounds are similar, the fluorescence spectra show distinct differences. Thus, the emission spectra of **14a,b** show Stokes shifts of 4100–6700 cm⁻¹ with low quantum yields both in solution and in the solid state. However, the more bulky compounds **14c–e** show markedly larger molar extinction coefficients and smaller bathochromic shifts compared to **14a,b**. For all compounds, we observe significantly more intense red-shifted fluorescence in the solid state compared to that in dichloromethane solutions. For the interpretation of the absorption properties TD-DFT studies were performed based on DFT geometry optimizations.

Received 5th March 2015,
Accepted 14th April 2015

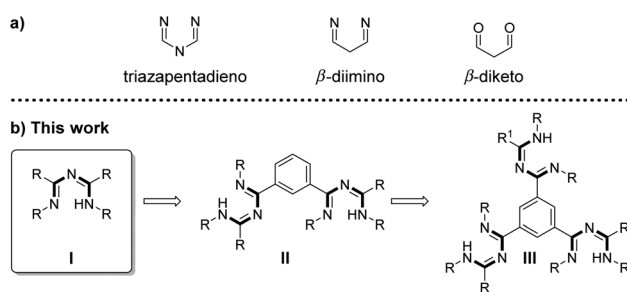
DOI: 10.1039/c5dt00908a

www.rsc.org/dalton

Introduction

Although 1,3,5-triazapentadienes are known since 1907,^{1–4} relatively little is known about their coordination chemistry compared to their carbon analogues β -diimine- and the well-known β -diketone ligands (Scheme 1).

1,3,5-Triazapentadienes are mostly used as ligands for transition metal ions,^{5,6} whereas coordination to main group elements, such as Al,⁷ Ga,⁸ Tl⁹ and boron, is currently underrepresented in the literature. Especially boron seems of interest to us, since boron–nitrogen compounds are known to exhibit intense fluorescence properties^{10,11} and are also used in modern applications like OLEDs.¹² In 1962 the first neutral 1 : 1 triazapentadiene–boron complex was synthesized by Milks *et al.*¹³ and, a decade later, Mikhailov *et al.* started to intensively study the synthesis of similar complexes.¹⁴ Since then, only a small number of research groups including ours^{15–18} have studied this class of neutral triazapentadiene–boron complexes. Species with such compositions and structural pro-



Scheme 1 (a) Backbone of a 1,3,5-triazapentadiene ligand and its carbon analogues. (b) Extension of the mono-triazapentadiene (I) to the benzene-centered bis- (II) and tris-triazapentadiene (III).

erties have not yet received intense attention, with some aza-boron-dipyridomethenes and aza-boron-diquinomethene systems showing the closest similarity to our compounds.¹⁹ In most of the studies, the photophysical properties are either not mentioned or are only of minor interest. This background encouraged us to look into this matter more closely.

In this article we describe (a) the synthesis and full structural characterization of a series of novel benzene-centered mono-, bis- and tris-1,3,5-triazapentadiene ligands and their di-phenylboron complexes featuring an increasing number of possible electronic and steric interactions, (b) their photophysical properties in solution and in the crystalline state as a function of the size of the complexes, which are (c) supported

^aOrganisch-Chemisches Institut, Westfälische Wilhelms-Universität, Corrensstr. 40, 48149 Münster, Germany. E-mail: wurthwe@uni-muenster.de

^bInstitute of Transformative Bio-molecules, and Department of Chemistry, Graduate School of Science, Nagoya University, Furo, Chikusa, Nagoya 464-8602, Japan

†Dedicated to the memory of Prof. Dr Paul von Ragué Schleyer.

‡Electronic supplementary information (ESI) available: Spectroscopic, crystallographic and quantum chemical details. CCDC 1011607–1011610. For ESI and crystallographic data in CIF or other electronic format see DOI: 10.1039/c5dt00908a



by extensive quantum chemical calculations for a better understanding of their electronic structures in the ground state and in the excited state. We were especially interested to know whether the accumulation of up to three boron complexes at the periphery of a benzene moiety exhibits intense electronic interactions of these photochemically active subgroups.

Results and discussion

Synthesis

Mono-triazapentadiene ligands **6a,b**: the synthesis of the hitherto unknown secondary triazapentadiene ligand **6a**, which bears two hydrogen atoms at the terminal nitrogen atom, was achieved by following a procedure developed by Heße *et al.*,^{4,5} whereas the novel tertiary triazapentadiene ligand **6b** (with one hydrogen atom at the terminal nitrogen atom) was synthesized by adapting a procedure of Häger *et al.* (Scheme 2).¹⁶

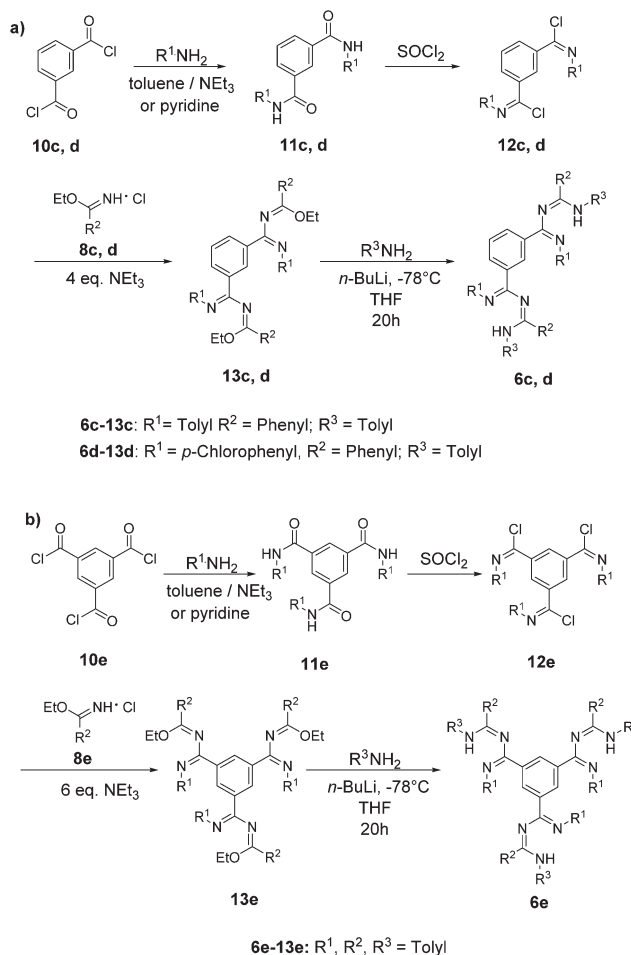
Bis- and tris-triazapentadiene ligands **6c–e**: the procedure used for **6b** is also the basis for the preparation of the bis-triazapentadienes **6c–d**²⁰ and the novel three-armed tris-triazapentadiene ligand **6e** (Scheme 3).

Because of the incomplete reaction and its distinct basic nature the free ligand **6e** is quite difficult to isolate. Therefore we decided to use the crude product **6e** for further reactions since we know from experience that the triazapentadiene boron compounds are readily purified by either recrystallization or *via* column chromatography on alumina oxide.^{15,21}

Boron complexes **14a–e**: the novel boron complexes derived from these ligands were synthesized by heating a solution of the respective triazapentadiene ligands **6a–e** with 1 to 3 equivalents of triphenylborane in toluene under reflux for 5 hours (Scheme 4).

After column chromatography on neutral alumina oxide, boron complexes **14a–e** featuring up to seven, thirteen and nineteen cyclic units in close chemical neighbourhood were obtained as yellow solids in yields from 47% to 77%. Recrystallization afforded crystalline solids, which have melting points in the range of 125–205 °C and show excellent thermal and chemical stability.

With these boron compounds in hand, a closer look into the structural properties and the influence of steric and elec-

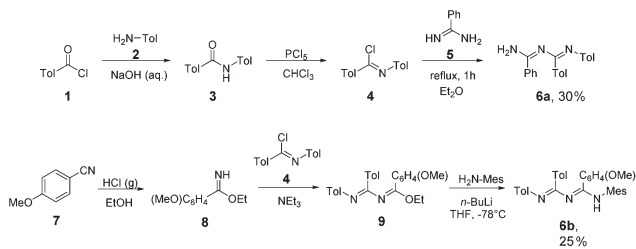


Scheme 3 Synthesis of (a) bis- (**6c, d**) and (b) tris-triazapentadiene ligands **6e**.

tronic effects on the photophysical properties of the triazapentadiene boron complexes were the next aims of this study.

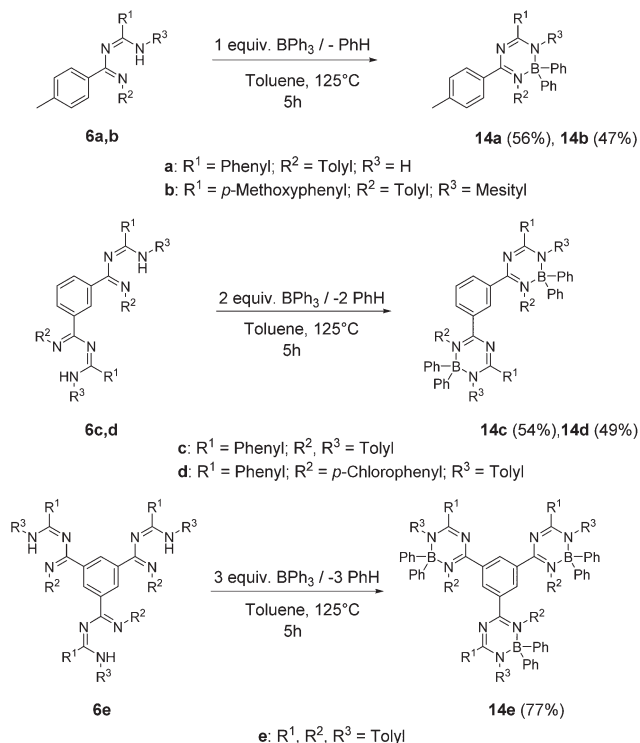
X-Ray structures

Single crystal X-ray diffraction analyses were carried out for **14a–c** and **14e** (Fig. 1; for **14a**, see Fig. S4, ESI†). For all three types of compounds substantial deviations from planarity are observed for the heterocyclic units due to the steric properties of the aryl substituents at the B, N, and C-positions and due to the sp^3 -hybridized boron atom (the dihedral angle C–N–B–N amounts to 43–51°). Furthermore the peripheral aryl substituents are strongly tilted with respect to the heterocycle (34–54° for the C-bound aryl groups, 44–64° for the N-bound aryl groups). Individual differences of the tilt angles may be due to the nature of the respective substitution patterns as well as due to crystal packing effects in the solid state. In general, our new boron compounds **14a–c** and **14e** may be described more or less as propeller shaped molecules, which was postulated to be a prerequisite to display the AIE effect in the solid state (see below).²²



Scheme 2 Synthetic pathways for secondary (**6a**) and tertiary (**6b**) mono-triazapentadiene ligands.





Scheme 4 Synthesis of the triazapentadiene–boron complexes **14a–e**.

Photophysical properties

Dichloromethane solutions of the boron complexes **14a,b** absorb light between $\lambda_{\text{abs}} = 250\text{--}450\text{ nm}$ with **14a** having its maximum at $\lambda_{\text{abs,max}} = 263\text{ nm}$ and **14b** at $\lambda_{\text{abs,max}} = 307\text{ nm}$. In both cases the longest absorption maximum occurs at $\lambda_{\text{abs}} = 353\text{ nm}$ in the form of a broad shoulder with molar extinction coefficients of $\epsilon_{353\text{ nm}} = 1000\text{ M}^{-1}\text{ cm}^{-1}\text{ L}$ for **14a** and $\epsilon_{353\text{ nm}} = 1300\text{ M}^{-1}\text{ cm}^{-1}\text{ L}$ for **14b**. They also exhibit blue emission in the range of $\lambda_{\text{em}} = 413\text{--}487\text{ nm}$ (Fig. 2, Table 1). In each case three bands are observed for **14a** at $\lambda_{\text{em}} = 413\text{ nm}$, 453 nm (fluorescence maximum) and 479 nm (very broad), for **14b** at $\lambda_{\text{em}} = 414\text{ nm}$ (fluorescence maximum), 446 nm and 487 nm (very broad). This leads to Stokes shifts of $\Delta\nu = 4100\text{ cm}^{-1}$ (**14a**) and $\Delta\nu = 4200\text{ cm}^{-1}$ (**14b**). The absolute quantum yields of the emissions are below one percent ($\Phi_{\text{F}} < 0.01$). This is consistent with the observation that the emission of **14a** and **14b** cannot be detected by the naked eye as shown in Fig. 2.

Interestingly, introducing an electron-donating group such as the *p*-methoxyphenyl group at the triazapentadiene unit (**14b**) has only a minor influence on the photophysical properties. As seen from the UV-spectra, the exchange of a single substituent at one of the many aryl groups has only a very little effect on the spectroscopic properties. The background for choosing different substitution patterns is mainly to demonstrate the synthetic versatility of our experimental method.

By increasing the steric bulk of this class of compounds by introducing a second (**14c,d**) and a third (**14e**) triazapenta-

diene boron unit, we attempted to decrease the conformational freedom of rotations of the ancillary substituents, thus making the possibility for radiative decay from the excited state dominant, which would result in an enhanced emission compared to the mono triazapentadiene boron compounds **14a,b**. These additional triazapentadiene boron units of compounds **14c–e** led in solution to relatively small bathochromic shifts but a strong increase of the molar extinction coefficients ϵ of the absorption (**14c,d**: $\lambda_{\text{abs}} = 365\text{ nm}$, $\epsilon_{365\text{ nm}} = 19\,000\text{ M}^{-1}\text{ cm}^{-1}\text{ L}$; **14e**: $\lambda_{\text{abs}} = 363\text{ nm}$, $\epsilon_{363\text{ nm}} = 26\,700\text{ M}^{-1}\text{ cm}^{-1}\text{ L}$; Table 1), which goes in line with the higher number of chromophores per volume in the bis- and tris-triazapentadiene boron complexes compared to the mono-compounds, resulting in more electronic transitions in the UV/vis-spectra. Similarly, the fluorescence maxima (**14c**: $\lambda_{\text{em,max}} = 542\text{ nm}$; **14d**: $\lambda_{\text{em,max}} = 539\text{ nm}$; **14e**: $\lambda_{\text{em,max}} = 517\text{ nm}$) are red-shifted compared to the mono triazapentadiene boron complexes **14a,b** (Fig. 3, Table 1). The Stokes shifts of these three compounds **14c–e** are significantly larger compared to those of **14a,b**. However, there is no enhancement of the absolute quantum yields, which are still below one percent ($\Phi_{\text{F}} < 0.01$). Thus, neither the differing substituent effects (**14b**, **14d**) nor the enhanced steric bulk (**14e**) result in a strong increase of the fluorescence of the complexes **14** in solution.

In contrast to the fluorescence of the solutions, the fluorescence of the crystalline materials **14a–e** is clearly visible to the naked eye upon irradiating the sample with a handheld UV-lamp as shown exemplarily in Fig. 4 for complexes **14a,c** and **e**.

The solid state emissions of the mono triazapentadiene boron complexes **14a** and **14b** are detected at $\lambda_{\text{em}} = 600\text{ nm}$ and $\lambda_{\text{em}} = 590\text{ nm}$, respectively. The bis-triazapentadiene boron complexes **14c,d** and the tris-triazapentadiene boron compound **14e** show their emission maximum in the solid state at the same wavelength ($\lambda_{\text{em}} = 560\text{ nm}$). Thus, all the emissions of the crystalline compounds are significantly red-shifted. While, as stated above, the quantum yields for **14a–e** in solution are below one percent, the absolute quantum yields in the crystalline state are at $\Phi_{\text{F}} = 0.02$ for **14a**, $\Phi_{\text{F}} = 0.03$ for **14b** and **14c**, $\Phi_{\text{F}} = 0.04$ for **14d** and $\Phi_{\text{F}} = 0.02$ for **14e** (Table 1).

This interesting behaviour of compounds **14a–e** indicates different emission properties in solution compared to those in the solid state. The formation of excimers and the aggregation induced emission effect (AIE), as first described in 2001 by the research group of B. Z. Tang,²² are possible explanations for these phenomena, which have to be studied in more detail before a conclusive interpretation can be made. Certainly, steric bulk and therefore hindered rotation of the aryl substituents are possible reasons which have to be considered.²³

To demonstrate the different emission properties in solution and in the solid state by an additional qualitative experiment, compound **14a** was dissolved in acetonitrile and water was added successively (Fig. 5).²⁴ As stated above, the acetonitrile solution of **14a** is not emitting light visible to the naked eye upon UV irradiation, but after addition of water **14a** precipitates due to its poor solubility in water and starts to



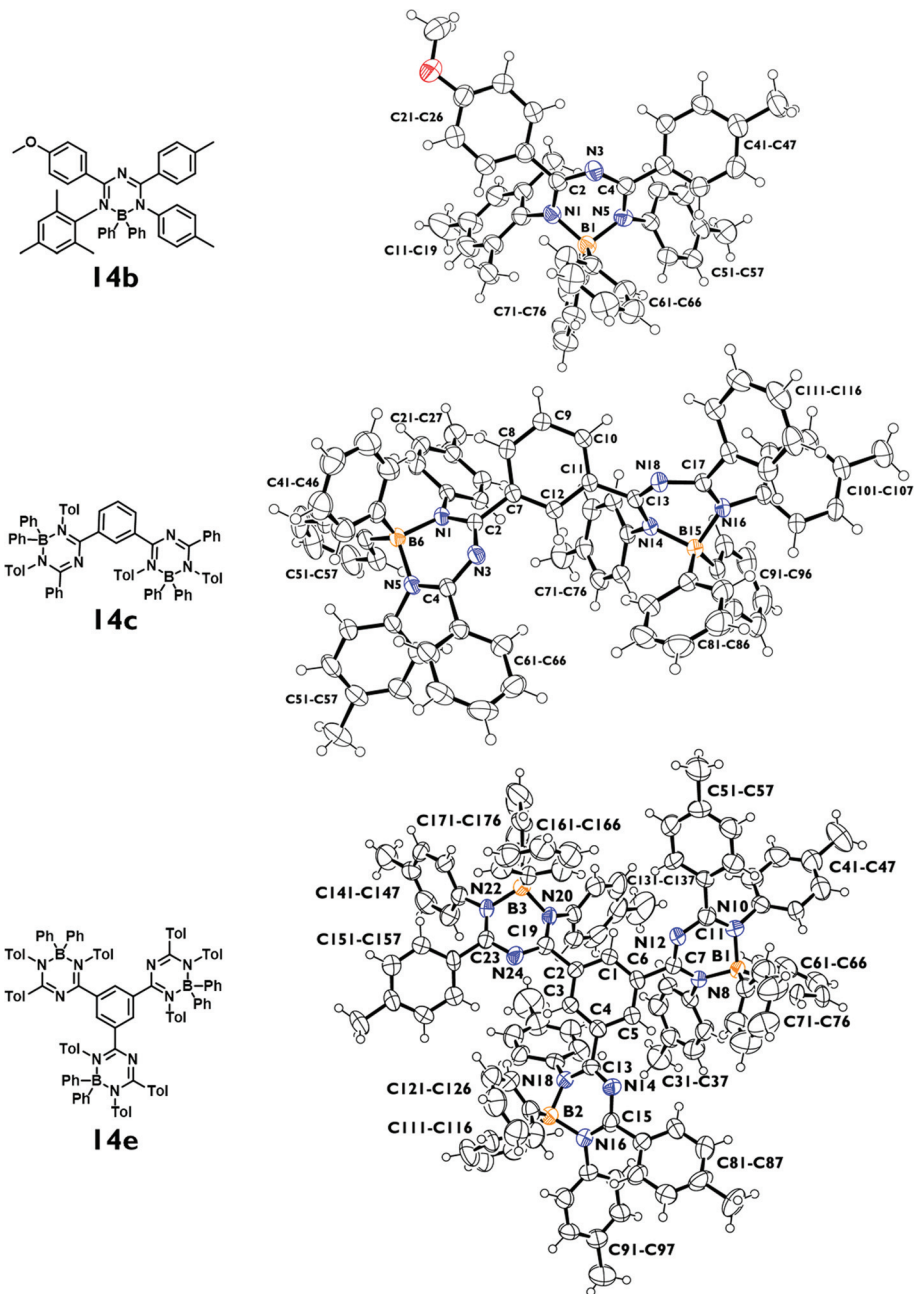


Fig. 1 ORTEP plots (thermal ellipsoids with 50% probability) of the molecular structures of **14b**, **c** and **e**. For detailed structural data for compounds **14a–c**, and **14e** see the ESI.†

emit yellow light. Worth noting is the considerable red-shift in the photoluminescence spectra of **14a** from $\lambda_{em} = 453$ nm for a solution in pure acetonitrile to $\lambda_{em} = 550$ nm for a suspension in a 1 : 1 acetonitrile/water mixture, which is possibly due to aggregation resulting in the formation of excimers. One should keep in mind that these spectra are to be treated qualitatively, since scatter light or other detection errors caused by particles are likely to occur.

Quantum chemical-DFT calculations

To investigate the electronic structures of the mono-, bis- and tris-triazapentadiene boron compounds, DFT geometry optimi-

zations of **14a–c** and **14e** at the B3LYP²⁵/def2-TZVP level using the GAUSSIAN 09 package of programs²⁶ for the gas phase without consideration of solvent effects were performed using the X-ray data as starting geometries. Subsequently, to study the light absorption of these molecules, excited singlet states and the respective transitions were evaluated using TD-DFT calculations considering each of 20 states (Gaussian 09: td = (root = 1, nstates = 20); see the ESI†).²⁷ The calculated and experimental UV/vis spectra including the oscillator strengths of the excited singlet states and the relevant Kohn–Sham molecular orbitals of **14a**, **14c** and **14e** are shown in Fig. 6–9. Additional data are given in the ESI.†



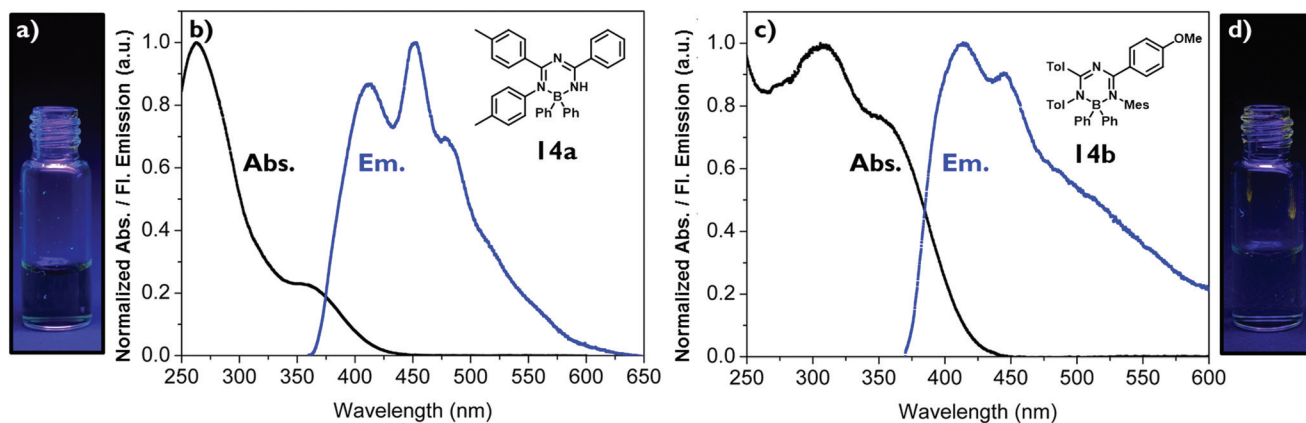


Fig. 2 (a) Photograph of compound **14a** in solution and (b) the normalized absorption and emission spectra of **14a** in CH_2Cl_2 . (c) Normalized absorption and emission spectra of **14b** in CH_2Cl_2 and (d) the photograph of compound **14b** in solution. Irradiation was performed with a UV lamp with a wavelength of 366 nm.

Table 1 Photophysical data of the boron compounds **14a–e**

Compound	$\lambda_{\text{abs}}^a/\text{nm}$	$\epsilon_{\text{max}}^b/\text{M}^{-1} \text{cm}^{-1} \text{L}$	$\lambda_{\text{em}}^c/\text{nm}$	$\Delta\nu^d/\text{cm}^{-1}$	Φ_{F}^e
14a	353	1000	453/600	4100	<0.01/0.02
14b	353	1300	414/590	4200	<0.01/0.03
14c	365	19 000	542/560	6100	<0.01/0.03
14d	365	19 000	539/560	6100	<0.01/0.04
14e	363	26 700	517/560	6700	<0.01/0.02

^a Longest wavelength absorption maxima recorded in dichloromethane using concentrations of about 10^{-5} M. ^b Molar extinction coefficient at the longest-wavelength absorption maximum. ^c Fluorescence maxima. Wavelengths are given for solution/solid. ^d Stokes shift in cm^{-1} as calculated from the longest wavelength absorption λ_{abs} and the shortest wavelength emission λ_{em} data (compare text and Fig. 2 and 3). ^e Absolute fluorescence quantum yield determined by a calibrated integration sphere system. Quantum yields are given for the solution/solid state.

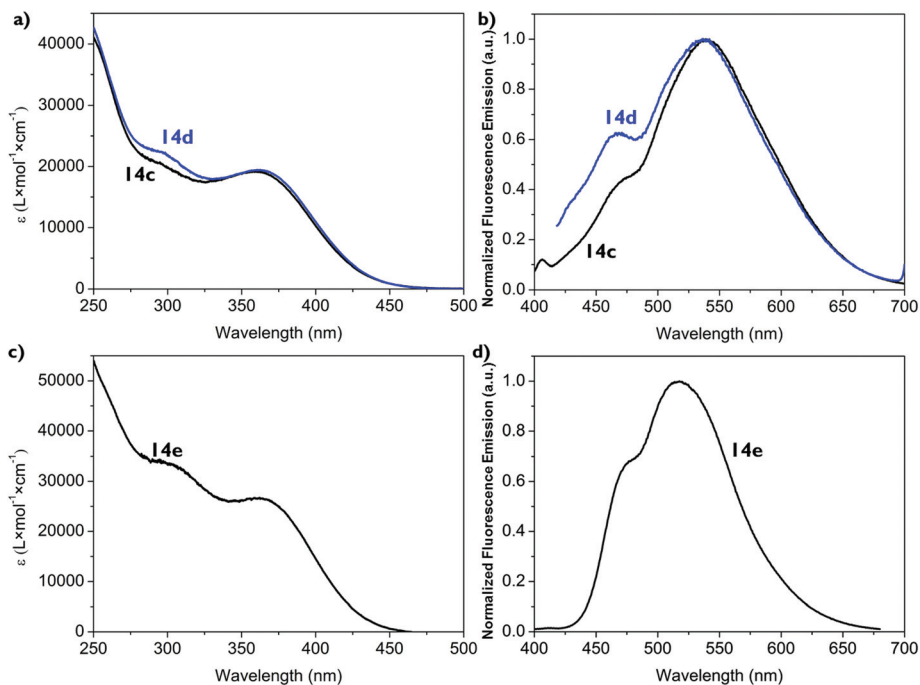


Fig. 3 (a) Absorption spectra of **14c**, **d** and (b) their normalized emission spectra. (c) Absorption spectrum of tris-triazapentadiene boron complex **14e** and (d) its normalized emission spectrum (10^{-5} M solutions in CH_2Cl_2).



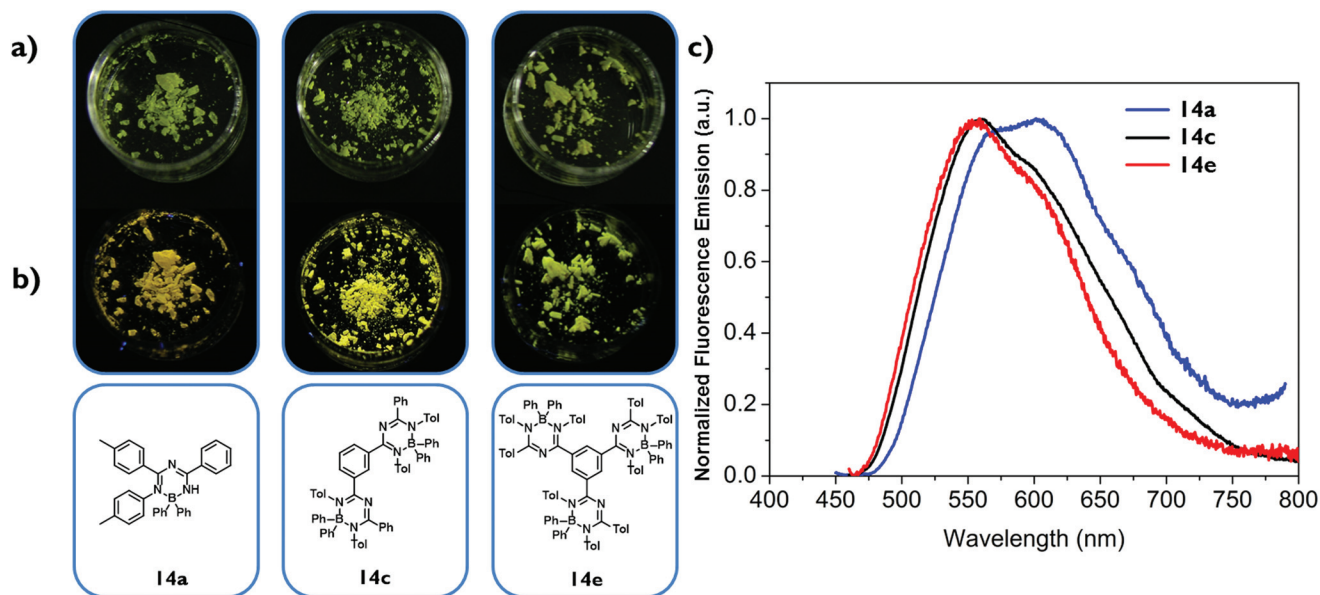


Fig. 4 Photographs of crystalline **14a**, **14c** and **14e** under (a) daylight and (b) in a dark room under UV irradiation. Irradiation was performed with a UV lamp with a wavelength of 366 nm. (c) Normalized emission spectra of **14a**, **14c**, and **14e** in the solid state.

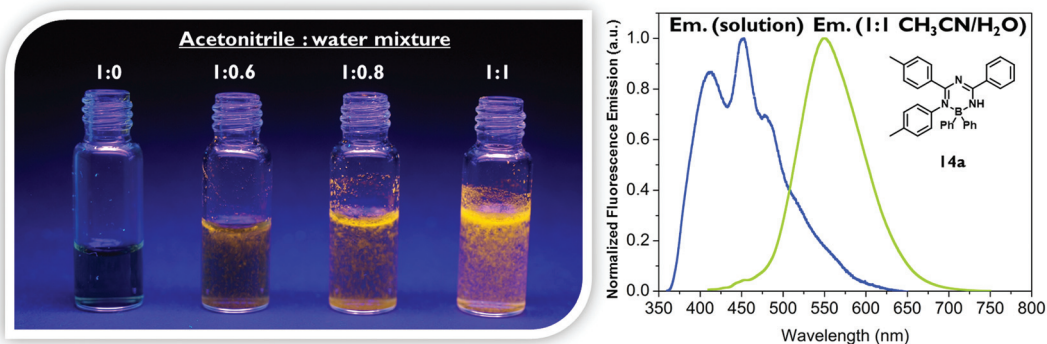


Fig. 5 Images of an acetonitrile/water (1:0–1:1) solution of **14a** during UV irradiation (left). Normalized photoluminescence spectrum of **14a** in a 1:0 (CH₃CN/H₂O) solution and a 1:1 (CH₃CN/H₂O) suspension (right). Irradiation was performed with a UV lamp with a wavelength of 366 nm.

For the mono-1,3,5-triazapentadiene–boron complex **14a**, the calculated UV/vis absorption spectrum matches quite well with the experimental one (Fig. 6). The absorption band at the longer wavelength, $\lambda_{\text{abs,calc}} = 343$ nm ($\lambda_{\text{abs,exp}} = 353$ nm), is described by the transitions involving S_1 , S_2 , S_3 and S_4 from the occupied molecular orbitals located mostly at the aryl substituents of the boron atom (HOMO–1, HOMO–2, HOMO–3) and at the nitrogen lone pairs as well as at the substituents of the triazapentadiene backbone (HOMO, HOMO–4) to the LUMO. Thus, the photochemistry of this system might be traced back to intramolecular charge transfer processes (ICT). The most intense absorption band at $\lambda_{\text{abs,calc}} = 273$ nm ($\lambda_{\text{abs,exp}} = 263$ nm) is predominantly described by the π – π^* transitions involving the states S_7 , S_9 and S_{13} , which can exclusively be traced back to excitations from occupied molecular orbitals at

the terminal substituents and the electron pairs at the nitrogen atoms of the triazapentadiene backbone (see the ESI[†]) into the LUMO which is concentrated at the triazapentadiene boron chelate.

For the bis-1,3,5-triazapentadiene–boron complex **14c** the experimentally observed absorption band at $\lambda_{\text{abs,exp}} = 359$ nm is reproduced by the calculations with a value of $\lambda_{\text{abs,calc}} = 365$ nm (Fig. 7). We assign it mainly to π – π^* transitions involving the states S_1 (HOMO–1 \rightarrow LUMO, HOMO \rightarrow LUMO, HOMO \rightarrow LUMO+1), S_2 (HOMO \rightarrow LUMO; HOMO–1 \rightarrow LUMO) and S_5 (HOMO–3 \rightarrow LUMO; (HOMO–4 \rightarrow LUMO) (see the ESI[†]).

The absorption spectrum of the tris-1,3,5-triazapentadiene–boron complex **14e** (Fig. 8) is qualitatively also similar to the spectra of **14a** and **14c** (Fig. 7). The calculated and the experi-



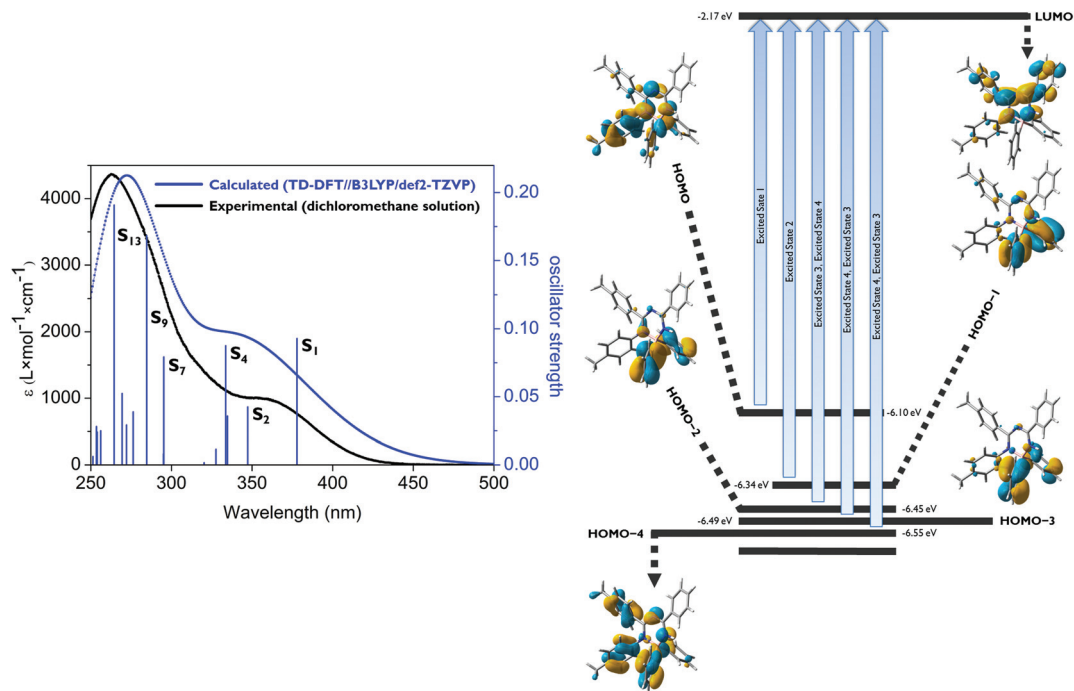


Fig. 6 The experimental (black, y1-axis) and calculated (blue) UV/VIS spectra of **14a** with the associated oscillator strength (y2-axis) (left). Transitions involving the excited states S_1 , S_2 , S_3 and S_4 and the relevant Kohn–Sham orbitals (right). For more detailed information see the ESI.†

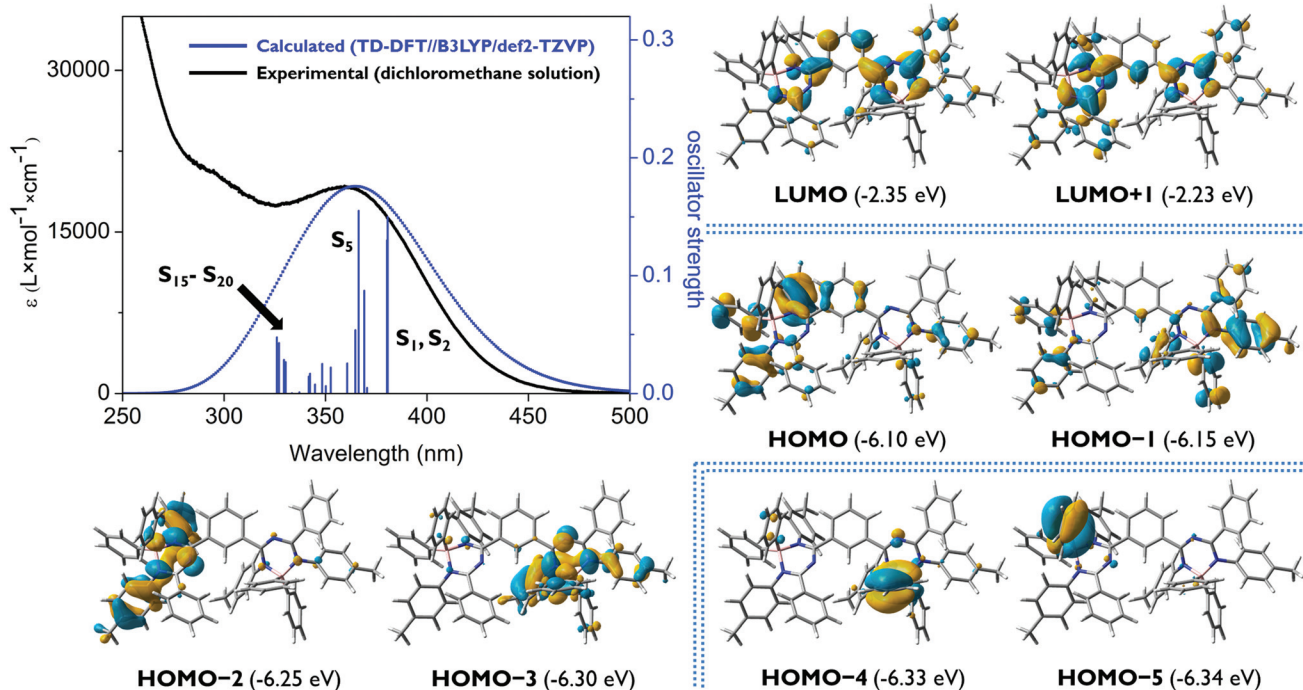


Fig. 7 The experimental (black, y1-axis) and calculated (blue) UV/VIS spectra of **14c** with the associated oscillator strength (y2-axis) (upper left). Kohn–Sham molecular orbitals of **14c**. The degree of degeneracy of the energy levels is clearly visible within the HOMO/HOMO–1, HOMO–2/HOMO–3 and HOMO–4/HOMO–5 pairs. For more detailed information, see the ESI.†



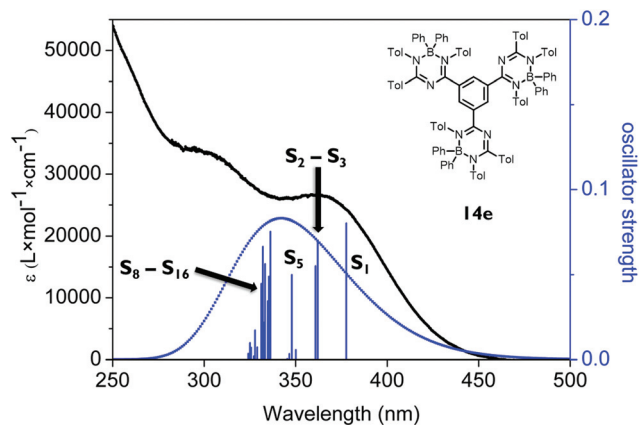


Fig. 8 The experimental UV/VIS spectrum (black, y1-axis) and the calculated excitation wavelengths of states S_1 – S_{20} for **14e** with the associated oscillator strength (y2-axis).

mental spectra show their longest wavelength absorption at $\lambda_{\text{abs,exp}} = 363$ nm and $\lambda_{\text{abs,calc}} = 345$ nm, which is represented by calculated transitions involving the states S_1 ($\lambda_{\text{abs,calc}} = 378$ nm), S_2 ($\lambda_{\text{abs,calc}} = 362$ nm), S_3 ($\lambda_{\text{abs,calc}} = 361$ nm) and S_5 ($\lambda_{\text{abs,calc}} = 348$ nm) involving usual π – π^* excitations from the three distinctly different orbitals HOMO, HOMO–1 and HOMO–2 located at the individual triazapentadiene subunits into their LUMO counterparts. The latter are characterized by participation of one (LUMO), two (LUMO+1, LUMO+3, LUMO+4) and three (LUMO+2) triazapentadiene boron units, which are electronically separated from each other. The absorption band at lower wavelength at $\lambda_{\text{abs,exp}} = 298$ nm is only partially represented by the accumulation of transitions involving the states S_8 – S_{20} ($\lambda_{\text{abs,calc}} = 335$ nm) concerning occu-

ried orbitals at the peripheral aryl substituents of the triazapentadiene boron units (e.g. HOMO–3, HOMO–4, HOMO–5) and the LUMO, LUMO+1 and LUMO+2 located at the three triazapentadiene–boron cores of the molecule (Fig. 9) (see the ESI† for additional Kohn–Sham molecular orbitals and calculation details). Not unexpectedly we noticed that the calculated gas phase absorption features of **14c** and **14e** do not match well with the experimental results at short wavelength when compared to **14a** and **14b**. Certainly, steric bulk and consequently more possible conformations and the lack of the solvent in the calculations are reasons for this observation.

As the experimental and calculated data clearly indicate, the mono-, the bis- and the tris-triazapentadiene boron compounds behave unexpectedly similarly with respect to their light absorption properties. This is indicated by the spectra and the orbital pictures and also by the similar HOMO/LUMO gaps which vary only in the range of $\Delta E_{\text{HOMO-LUMO}} = 3.75$ – 3.93 eV. Thus, due to the heavy steric hindrance, all three systems exhibit only limited delocalization of electrons throughout the molecule. In contrast, as shown above, the fluorescence properties (emission maxima and Stokes shifts) of these three types of boron compounds differ significantly, especially in the solid state. This indicates the importance of steric properties caused by intra- and intermolecular interactions.

Experimental section

General procedures

Compounds **1–3**, **5** and **7** are commercially available. The bis-triazapentadiene ligands **6c** and **6d** including their precursors (**11c–13c**, **11d–13d**) were synthesized following a literature procedure.²⁰ Melting points are uncorrected. Nuclear magnetic

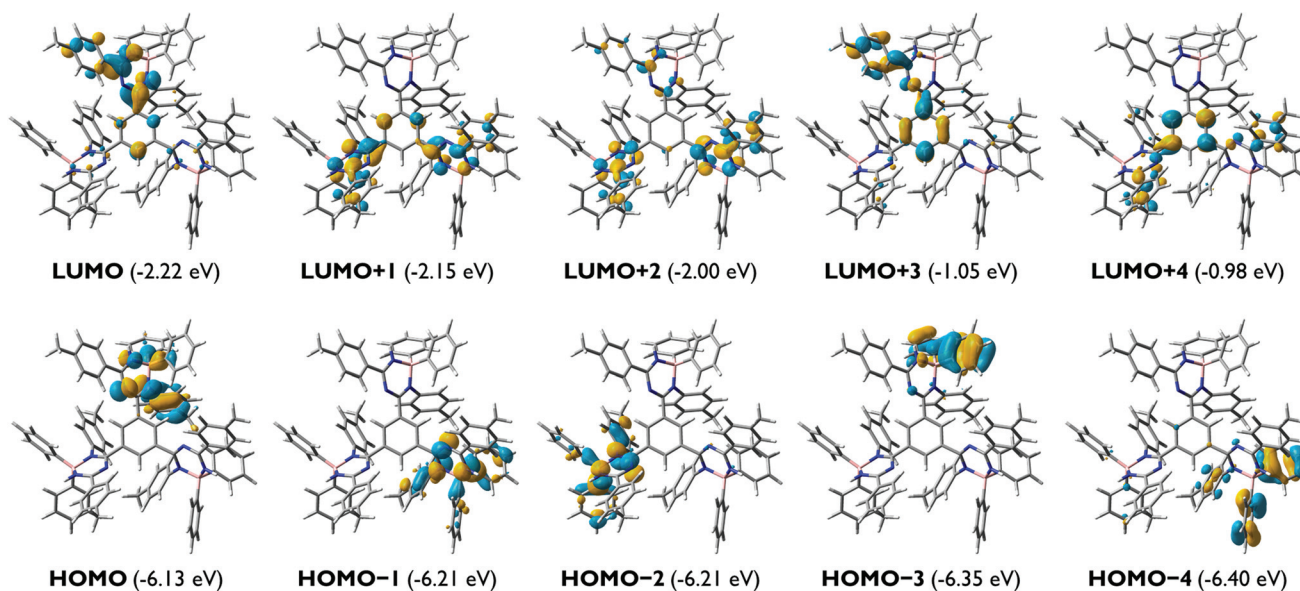


Fig. 9 Kohn–Sham molecular orbital pictures of compound **14e**.



resonance spectroscopy (^1H , ^{13}C , ^{11}B , ^{19}F) was performed on superconductive spectrometers: 300 MHz (^1H : 300.1 MHz, ^{13}C : 75.5 MHz, ^{19}F : 282.4 MHz, ^{11}B : 96.3 MHz), 400 MHz (^1H : 400.1 MHz, ^{13}C : 100.6 MHz), 500 MHz (^1H : 499.9 MHz, ^{13}C : 125.7 MHz, ^{19}F : 470.3 MHz, ^{11}B : 160.4 MHz) and 600 MHz (^1H : 599.8 MHz, ^{13}C : 150.8 MHz, ^{19}F : 564.4 MHz, ^{11}B : 192.4 MHz). ^1H NMR and ^{13}C NMR: chemical shifts δ are given relative to TMS and referenced to the solvent signal. ^{19}F NMR: chemical shifts δ are given relative to CFCl_3 (external reference), ^{11}B NMR: chemical shifts δ are given relative to $\text{BF}_3\cdot\text{OEt}_2$ (external reference). All signals in the ^1H NMR and ^{13}C spectra were assigned on the basis of relative intensities, coupling constants, and GCOSY, GHSQC, GHMBC, 1D-COSY and 1D-NOE experiments. Mass spectra were recorded on a micrOTOF using electron spray ionization. UV/VIS absorption spectra were recorded with a resolution of 0.2 nm to 0.5 nm. If not stated otherwise, dilute solutions with concentrations about 10^{-5} M in a 1 cm square quartz cell in degassed dichloromethane were used. Fluorescence lifetimes were measured with a Picosecond Fluorescence Measurement System equipped with a picosecond light pulser (excitation wavelength 377 nm with a repetition rate of 10 Hz). Absolute fluorescence quantum yields were determined with a calibrated integrating sphere system. X-Ray diffraction (for more information please see the ESI ‡): Data sets were collected with a Nonius KappaCCD diffractometer or a Rigaku CCD diffractometer with a rotating anode generator. The programs used: data collection, COLLECT (R. W. W. Hooft, Bruker AXS, 2008, Delft, The Netherlands) and CrystalClear (Rigaku Corp., 2000); data reduction Denzo-SMN (Z. Otwinowski, W. Minor, *Methods Enzymol.*, 1997, 276, 307–326); absorption correction, Denzo (Z. Otwinowski, D. Borek, W. Majewski, W. Minor, *Acta Crystallogr., Sect. A: Fundam. Crystallogr.*, 2003, 59, 228–234); structure solution SHELXS-97 (G. M. Sheldrick, *Acta Crystallogr., Sect. A: Fundam. Crystallogr.*, 1990, 46, 467–473); structure refinement SHELXL-97 (G. M. Sheldrick, *Acta Crystallogr., Sect. A: Fundam. Crystallogr.*, 2008, 64, 112–122) and graphics, XP (Bruker AXS, 2000). R -values are given for the observed reflections, and wR_2 values are given for all reflections. Supplementary crystallographic data for **14a**, **14b**, **14c** and **14e** CCDC 1011607–1011610 are given in the ESI. ‡

Synthesis of the starting materials and the mono- and tris-triazapentadiene ligands

Synthesis of ligand 6a. A solution of imidoyl chloride **4**²⁸ (8.44 g, 34.6 mmol, 1.0 equiv.) in diethyl ether (40 mL) was added dropwise to a suspension of benzamidine (4.16 g, 34.6 mmol, 1.0 equiv.) in diethyl ether (20 mL). The reaction mixture was stirred for 2 h at room temperature and for 1 h under refluxing conditions. The resulting precipitate was filtered off and sonicated in hot water to remove benzamidine hydrochloride. The residual triazapentadiene hydrochloride was separated and converted into **6a** by adding a sodium hydroxide solution (2 N, 50 mL). The solution was extracted with dichloromethane several times until no solid remains. The combined organic layers were dried with magnesium

sulfate. Removing the solvent *in vacuo* gave compound **6a** as a yellow solid in 30% (3.38 g) yield: mp 118 °C. ^1H NMR (300 MHz; CDCl_3): δ 7.93 (d, 2H, ArH), 7.67 (m, 2H, ArH), 7.43 (m, 3H, ArH), 7.23 (d, 2H, ArH), 6.98 (m, 4H ArH), 4.83 (br, 2H, NH_2), 2.40 (s, 3H, $-\text{CH}_3$), 2.27 (s, 3H, $-\text{CH}_3$) ppm. ^{13}C NMR (75 MHz; CDCl_3): δ 161.0, 152.6 ($\text{C}=\text{N}$), 147.7, 141.1, 134.4 (C_q), 132.5, 131.1, 129.6, 129.2, 128.8, 128.6, 128.1, 126.9, 121.4 (C_{Ar}), 21.3, 20.7 (CH_3) ppm. Anal. Calcd for $\text{C}_{22}\text{H}_{21}\text{N}_3$: C, 80.71; H, 6.46; N, 12.83. Found: C, 80.68; H, 6.40; N, 12.88.

Synthesis of ligand 6b. A solution of 2,4,6-trimethylaniline (1.1 mL, 7.8 mmol, 1.0 equiv.) in dry tetrahydrofuran (15 mL) was cooled down to -78 °C and an equimolar amount of *n*-butyl lithium was added dropwise. After the reaction mixture was stirred for 10 min, imidate **9** (3.1 g, 7.8 mmol, 1.0 equiv.) was slowly added and stirred overnight at room temperature. The organic layer was washed with saturated sodium chloride solution (3×20 mL) before being dried with magnesium sulfate. The solvent was removed *in vacuo* and the crude product was recrystallized from a pentane/tetrahydrofuran to obtain **6b** as yellow crystals in 25% (900 mg) yield: mp 176 °C. ^1H NMR (400 MHz; C_6D_6): δ 7.52–7.42 (m, 2H, ArH), 7.05–7.02 (m, 4H, ArH), 6.92–6.80 (m, 4H, ArH), 6.74–6.66 (m, 4H, ArH), 6.15 (br, 1H, NH), 3.82 (s, 3H, $-\text{OCH}_3$), 2.32 (s, 3H, $-\text{CH}_3$), 2.30 (s, 3H, $-\text{CH}_3$), 2.29 (s, 3H, $-\text{CH}_3$), 2.21 (s, 6H, Mes- CH_3 , *ortho*) ppm. ^{13}C NMR (100 MHz; C_6D_6): δ 161.4, 159.3 ($\text{C}=\text{N}$), 144.2, 142.1, 140.5, 136.8 (C_q), 136.6 (C_{Ar}), 135.3, 134.7, 134.5, 133.0 (C_q), 132.9, 131.0, 130.1, 129.4, 129.3, 129.1, 128.9, 127.3, 126.9, 113.6 (C_{Ar}), 55.5 ($-\text{OCH}_3$), 21.6, 21.1, 21.0, 20.8 (CH_3) ppm. HRMS (ESI): calcd for $\text{C}_{32}\text{H}_{34}\text{N}_3\text{O}$ ($[\text{M} + \text{H}]^+$) 476.2696, observed 476.2695.

Synthesis of ligand 6c. A solution of *p*-toluidine (2.73 g, 25.5 mmol, 7.5 equiv.) in dry tetrahydrofuran was cooled down to -78 °C and *n*-butyl lithium (15.93 mL, 1.6 M, 25.5 mmol, 7.5 equiv.) was added dropwise. After stirring the solution for 30 min, a solution of compound **13e** (3.10 g, 3.4 mmol, 1.0 equiv.) in dry tetrahydrofuran was added slowly. After removal of the acetone/ CO_2 -bath, the reaction mixture was stirred overnight and quenched with water afterwards. The crude product was filtered through deactivated silica (80% cyclohexane, 20% ethyl acetate, $R_f = 0.19$) and directly used for further reactions after confirmation of the mass *via* HRMS. HRMS (ESI): calcd for $\text{C}_{75}\text{H}_{70}\text{N}_9$ ($[\text{M} + \text{H}]^+$) 1096.5749, observed 1096.5735.

Synthesis of *N*-imidoylimidate 9. Ethyl 4-methoxybenzimidate hydrochloride²⁹ (5.6 g, 30.0 mmol, 1.0 equiv.) was suspended in dry dichloromethane (20 mL) and triethylamine (2.8 mL, 20.0 mmol, 2.0 equiv.) was added dropwise. After stirring for 1 h the reaction vessel was cooled down to 0 °C and imidoyl chloride **4**²⁸ (7.3 g, 30.0 mmol, 1.0 equiv.) was added slowly. After the reaction mixture was stirred for 20 h, the precipitate was filtered off and washed several times with warm diethyl ether. The filtrate was evaporated and the crude product was purified by column chromatography on silica yielding **9** as yellow oil which was slowly crystallizing, giving **9** in 56% yield as a yellow solid: mp 85 °C. ^1H NMR (300 MHz; CDCl_3): δ 7.96–7.87 (m, 2H, ArH), 7.40–7.32 (m, 2H, ArH),



7.23–7.16 (m, 2H, ArH), 6.96–6.87 (m, 2H, ArH), 6.75–6.67 (m, 2H, ArH), 6.62–6.54 (m, 2H, ArH), 4.26 (q, $J_{\text{HH}} = 7.0$ Hz, 2H, $\text{H}_3\text{CCH}_2\text{O}-$), 3.74 (s, 3H, $-\text{OCH}_3$), 2.38 (s, 3H, $-\text{CH}_3$), 2.24 (s, 3H, $-\text{CH}_3$), 1.31 (t, $J_{\text{HH}} = 7.1$ Hz, 3H, $\text{H}_3\text{CCH}_2\text{O}-$) ppm. ^{13}C NMR (75 MHz; CDCl_3): δ 161.7 ($-\text{O}-\text{C}=\text{N}$), 158.5 ($=\text{N}-\text{C}=\text{N}$), 156.6 (C_q-OCH_3), 147.5, 140.7, 133.7, 131.8, 130.0 (C_q), 129.2, 128.9, 128.1, 124.0, 121.7, 113.7 (C_{Ar}), 63.0 ($\text{H}_3\text{CCH}_2\text{O}-$), 55.4 ($-\text{OCH}_3$), 21.6, 21.1 ($-\text{CH}_3$), 14.5 ($\text{H}_3\text{CCH}_2\text{O}-$) ppm. HRMS (ESI): calcd for $\text{C}_{24}\text{H}_{27}\text{N}_2\text{O}_2$ ($[\text{M} + \text{H}]^+$) 387.2067, observed 387.2067.

Synthesis of amide 11e. This compound was prepared by modification of a literature procedure.^{30,31} A suspension of *p*-toluidine (16.1 g, 150.0 mmol, 5.0 equiv.) in dry toluene (200 mL) and triethylamine (12.6 mL, 90.0 mmol, 3.0 equiv.) was cooled to 0 °C. Then a solution of trimesoyl chloride (8.0 g, 30.0 mmol, 1.0 equiv.) in toluene (100 mL) was added dropwise over a period of 1 h. The solution was then stirred vigorously for 12 h before the solvent was evaporated *in vacuo*. The residue was dissolved in dichloromethane and washed with water (3 × 100 mL). Finally the organic layer was dried over MgSO_4 and the solvent was removed to give **11e** as a colorless solid in 95% (13.5 g) yield: mp 299 °C (297–298 °C³¹). ^1H NMR (300 MHz; $\text{C}_2\text{D}_6\text{SO}$): δ 10.53 (s, 3H, NH), 8.69 (s, 3H, ArH), 7.72 (d, $J_{\text{HH}} = 8.4$ Hz, 6H, ArH), 7.20 (d, $J_{\text{HH}} = 8.3$ Hz, 6H, ArH), 2.30 (s, 9H, $-\text{CH}_3$) ppm. ^{13}C NMR (75 MHz; $\text{C}_2\text{D}_6\text{SO}$): δ 164.4 ($\text{C}=\text{O}$), 136.5, 135.6, 133.0 (C_q), 129.7, 129.2, 120.4 (C_{Ar}), 20.6 ($-\text{CH}_3$) ppm. HRMS (ESI): calcd for $\text{C}_{30}\text{H}_{27}\text{N}_3\text{O}_3\text{Na}$ ($[\text{M} + \text{Na}]^+$) 500.1945, observed 500.1945.

Synthesis of imidoyl chloride 12e. Amide **11e** (15.4 g, 32.3 mmol, 1.0 equiv.) was added in several portions to thionyl chloride (70.1 mL, 967.5 mmol, 30.0 equiv.) while stirring. The brown solution was then stirred for 3 h under refluxing conditions and the resulting SO_2 and HCl were removed under reduced pressure. The yellowish solid was recrystallized from a tertiary butyl methyl ether/dichloromethane 1 : 1 mixture yielding **12e** as a yellow crystalline compound in 71% (12.2 g) yield: mp 133 °C. ^1H NMR (300 MHz; CD_2Cl_2): δ 9.08 (s, 3H, ArH), 7.36–7.13 (m, 6H, ArH), 7.12–6.93 (m, 6H, ArH), 2.40 (s, 9H, $-\text{CH}_3$) ppm. ^{13}C NMR (75 MHz; CD_2Cl_2): δ 145.0 ($-\text{Cl}-\text{C}=\text{N}$), 141.2, 137.2, 136.2 (C_q), 133.3, 130.1, 121.1 (C_{Ar}), 21.3 ($-\text{CH}_3$) ppm.

Synthesis of *N*-imidoylimidate 13e. Ethyl 4-methylbenzimidate hydrochloride **8**³² (9.1 g, 45.6 mmol, 3.0 equiv.) was suspended in dry dichloromethane (20 mL) and triethylamine (12.7 mL, 91.2 mmol, 6.0 equiv.) was added dropwise. At –15 °C, imidoyl chloride **12e** (8.1 g, 15.2 mmol, 1.0 equiv.) was slowly added to the solution. After the reaction mixture was stirred for 20 h, the precipitate was filtered off and washed several times with warm diethyl ether. The filtrate was evaporated and the crude product was purified by column chromatography on deactivated silica with 90% cyclohexane and 10% ethyl acetate ($R_f = 0.20$) yielding **13e** as a yellow oil in 22% (3.1 g) yield: ^1H NMR (400 MHz; CD_2Cl_2): δ 8.64 (s, 3H, ArH), 7.22–7.16 (m, 6H, ArH), 7.02–6.94 (m, 12H, ArH), 6.68–6.61 (m, 6H, ArH), 4.32 (dq, $J_{\text{HH}} = 11.8, 7.1$ Hz, 6H, $-\text{O}-\text{CH}_2\text{CH}_3$), 2.29 (s, 9H, $-\text{CH}_3$), 2.27 (s, 9H, $-\text{CH}_3$), 1.36 (dt, $J_{\text{HH}} = 8.8, 7.1$

Hz, 9H, $-\text{O}-\text{CH}_2\text{CH}_3$) ppm. ^{13}C NMR (100 MHz; CD_2Cl_2): δ 158.1, 157.5 ($\text{C}=\text{N}$), 147.6, 142.2, 137.4, 132.7 (C_q), 129.4, 129.3, 128.3, 122.1 (C_{Ar}), 63.7 ($-\text{O}-\text{CH}_2\text{CH}_3$), 21.7, 21.1 ($-\text{CH}_3$), 14.6 ($-\text{O}-\text{CH}_2\text{CH}_3$) ppm. HRMS (ESI): calcd for $\text{C}_{60}\text{H}_{61}\text{N}_6\text{O}_3$ ($[\text{M} + \text{H}]^+$) 913.4800, observed 913.4806.

Synthesis of boron compounds 14a–14e based on mono-, bis- and tris-triazapentadiene ligands 6

Synthesis of boron complex 14a. A Schlenk flask connected to a reflux condenser under an argon atmosphere was charged with triphenylborane (307 mg, 1.5 mmol, 1.0 equiv.) and triazapentadiene **6a** (488 mg, 1.5 mmol, 1.0 equiv.). After adding dry toluene (20 mL) to the solids the solution was refluxed for 3 h. After cooling down the reaction mixture the solvent was removed *in vacuo* and the crude product was subjected to column chromatography on neutral alumina with 99% cyclohexane and 1% ethyl acetate ($R_f = 0.29$). Title compound **14a** was obtained as a yellow crystalline solid in 45% (322 mg) yield: mp 205 °C. ^1H NMR (300 MHz; C_6D_6): δ 7.92–7.85 (m, 4H, ArH), 7.74–7.65 (m, 4H, ArH), 7.42–7.33 (m, 4H, ArH), 7.29–7.20 (m, 2H, ArH), 7.12–7.02 (m, br, 2H, NH, ArHH), 7.01–6.93 (m, 2H, ArH), 6.89–6.83 (m, 2H, ArH), 6.81–6.72 (m, 2H, ArH), 6.48–6.42 (m, 2H, ArH), 1.85 (s, 3H, $-\text{CH}_3$), 1.70 (s, 3H, $-\text{CH}_3$) ppm. ^{13}C NMR (75 MHz; C_6D_6): δ 168.4, 163.3 ($\text{C}=\text{N}$), 143.1, 140.3, 135.9, 135.7 (C_q), 134.9 (C_{Ar}), 134.6 (C_q), 133.1, 132.3, 131.3, 129.2, 129.1, 129.0, 127.0 (C_{Ar}), 21.5, 21.0 ($-\text{CH}_3$) ppm. ^{11}B NMR (96 MHz; C_6D_6): δ 0.4 (s, B_{quart} , $\nu_{1/2} \sim 910$ Hz) ppm. HRMS (ESI): calcd for $\text{C}_{34}\text{H}_{31}\text{N}_3\text{B}$ ($[\text{M} + \text{H}]^+$) 492.2611, observed 492.2603. UV/VIS (dichloromethane): λ_{abs} (shape, $\tilde{\nu}$, ϵ) = 353 nm (sh, 28 329 cm^{-1} , 1000 $\text{L mol}^{-1} \text{cm}^{-1}$), 263 nm (p, 38 023 cm^{-1} , 4400 $\text{L mol}^{-1} \text{cm}^{-1}$). Fluorescence (dichloromethane): λ_{em} (shape, $\tilde{\nu}$) = 479 nm (p, 20 876 cm^{-1}), 453 nm (p, 22 075 cm^{-1}), 412 nm (p, 24 272 cm^{-1}). Absolute quantum yield (dichloromethane): $\Phi_{\text{F}} < 1\%$.

Synthesis of boron complex 14b. A Schlenk flask connected to a reflux condenser under an argon atmosphere was charged with triphenylborane (207 mg, 0.9 mmol, 1.0 equiv.) and triazapentadiene **6b** (404 mg, 0.9 mmol, 1.0 equiv.). After adding dry toluene (20 mL) to the solids the solution was refluxed for 3 h. After cooling down the reaction mixture the solvent was removed *in vacuo* and the crude product was subjected to column chromatography on neutral alumina with 95% cyclohexane and 5% ethyl acetate ($R_f = 0.22$). Title compound **14b** was obtained as a yellow crystalline solid in 47% (280 mg) yield: mp 125 °C. ^1H NMR (300 MHz; C_6D_6): δ 8.26–8.18 (m, 2H, ArH), 7.91–7.83 (m, 4H, ArH), 7.76–7.68 (m, 2H, ArH), 7.23–7.17 (m, 5H, ArH), 7.15–7.04 (m, 3H, ArH), 6.73–6.67 (m, 2H, ArH), 6.64–6.53 (m, 4H, ArH), 6.35 (s, 2H, ArH), 3.06 (s, 3H, $-\text{OCH}_3$), 2.33 (s, 6H, $(-\text{CH}_3)_2$), 1.81 (s, 6H, $(-\text{CH}_3)_2$), 1.80 (s, 3H, $-\text{CH}_3$) ppm. ^{13}C NMR (75 MHz; C_6D_6): δ 168.5, 167.8 ($\text{C}=\text{N}$), 162.7, 143.4, 142.8, 140.7 (C_q), 136.4 (C_{Ar}), 136.2, 136.0, 135.6, 135.3 (C_q), 133.5, 131.8, 130.1, 129.5, 129.1, 129.2, 127.0, 126.6, 114.0 (C_{Ar}), 55.0 ($-\text{OCH}_3$), 21.5, 21.4, 21.1, 21.0 ($-\text{CH}_3$) ppm. ^{11}B NMR (96 MHz; C_6D_6): δ 2.9 (s, B_{quart} , $\nu_{1/2} \sim 960$ Hz) ppm. HRMS (ESI): calcd for $\text{C}_{44}\text{H}_{43}\text{N}_3\text{OB}$ ($[\text{M} + \text{H}]^+$) 640.3501, observed 640.3507. UV/VIS (dichloromethane): λ_{abs}



(shape, $\tilde{\nu}$, ϵ) = 353 nm (sh, 28 329 cm⁻¹, 1300 L mol⁻¹ cm⁻¹), 307 nm (p, 35 573 cm⁻¹, 1800 L mol⁻¹ cm⁻¹). Fluorescence (dichloromethane): λ_{em} (shape, $\tilde{\nu}$) = 494 nm (sh, 20 243 cm⁻¹), 447 nm (p, 22 371 cm⁻¹), 414 nm (p, 24 155 cm⁻¹). Absolute quantum yield (dichloromethane): Φ_F = <1%. Absolute quantum yield (crystalline): Φ_F = 3%.

Synthesis of boron complex 14c. A flask under an inert atmosphere was charged with triphenylborane (412 mg, 1.70 mmol, 2.0 equiv.) and bis-triazapentadiene **6c**²⁰ (619 mg, 0.85 mmol, 1.0 equiv.). After adding dry toluene, the reaction mixture was heated under refluxing conditions for 4 h. After that time, the solvent was removed under reduced pressure and the crude product was subjected to column chromatography on neutral alumina with 90% cyclohexane and 10% ethyl acetate (R_f = 0.44) to furnish the bis-triazapentadiene boron compound **14c** in 54% (485 mg) yield: mp 187 °C. ¹H NMR (600 MHz, CD₂Cl₂): δ 8.00 (t, J_{HH} = 1.9 Hz, 1H, -N=C_q-C_q-CH-C_q), 7.63–7.59 (m, 4H, ArH), 7.55–7.50 (m, 8H, B-ArH), 7.41 (dd, J_{HH} = 7.8 Hz, J_{HH} = 1.9 Hz, 2H, -N=C_q-C_q-CH-CH-CH-C_q), 7.35–7.31 (m, 2H, ArH), 7.29–7.23 (m, 4H, ArH), 7.20–7.10 (m, 12H, B-ArH), 6.99 (t, J_{HH} = 7.8 Hz, 1H, -N=C_q-C_q-CH-CH-CH-C_q), 6.69 (ddt, J_{HH} = 8.9, 7.4, 0.8 Hz, 8H, ArH), 6.65–6.60 (m, 4H, ArH), 6.51–6.46 (m, 4H, ArH), 2.13 (s, 6H, -CH₃), 2.11 (s, 6H, -CH₃) ppm. ¹³C NMR (150 MHz, CD₂Cl₂): δ 166.9, 165.9 (C=N), 147.9 (B-C_q), 142.1, 142.0, 137.5, 136.9 (C_q), 135.9, 135.8 (C_q-CH₃), 135.3 (B-C_{Ar}), 133.4, 131.7 (C_{Ar,centralBenzene}), 130.7, 130.1, 128.8, 128.7, 128.5, 128.4, 128.1 (C_{Ar}), 127.2 (C_{Ar,centralBenzene}), 127.0, 126.1 (B-C_{Ar}), 21.0, 20.9 (-CH₃) ppm. ¹¹B NMR (192 MHz, CD₂Cl₂): δ 2.4 (s, B_{quart} , $\nu_{1/2}$ ~ 740 Hz) ppm. HRMS (ESI): calcd for C₇₄H₆₃B₂N₆ ([M + H]⁺) 1057.5316, observed 1057.5307. UV/VIS (dichloromethane): λ_{abs} (shape, $\tilde{\nu}$, ϵ) = 365 nm (p, 27 397 cm⁻¹, 19 000 L mol⁻¹ cm⁻¹), 297 nm (sh, 33 670 cm⁻¹, 20 700 L mol⁻¹ cm⁻¹). Fluorescence (dichloromethane): λ_{em} (shape, $\tilde{\nu}$) = 538 nm (p, 18 587 cm⁻¹), 469 nm (p, 21 322 cm⁻¹). Absolute quantum yield (dichloromethane): Φ_F = <1%. Absolute quantum yield (crystalline): Φ_F = 3%.

Synthesis of boron complex 14d. A flask under an inert atmosphere was charged with triphenylborane (430 mg, 1.8 mmol, 2.0 equiv.) and bis-triazapentadiene **6d**²⁰ (685 mg, 0.9 mmol, 1.0 equiv.). After adding dry toluene, the reaction mixture was heated under refluxing conditions for 4 h. After that time, the solvent was removed under reduced pressure and the crude product was subjected to column chromatography on neutral alumina with 90% cyclohexane and 10% ethyl acetate (R_f = 0.35) to furnish the bis-triazapentadiene boron compound **14d** as a yellow solid in 49% (479 mg) yield: mp 120 °C. ¹H NMR (600 MHz, CD₂Cl₂): δ 7.92 (td, J_{HH} = 0.5 Hz, 1H, -N=C_q-C_q-CH-C_q), 7.60–7.55 (m, 4H, ArH), 7.52–7.47 (m, 8H, B-ArH), 7.39–7.33 (m, 4H, ArH), 7.31–7.24 (m, 4H, ArH), 7.19–7.07 (m, 12H, B-ArH), 6.98 (td, J_{HH} = 7.7 Hz, J_{HH} = 0.5 Hz, 1H, -N=C_q-C_q-CH-CH-CH-C_q), 6.84–6.78 (m, 4H, ArH), 6.70–6.65 (m, 4H, ArH), 6.65–6.61 (m, 4H, ArH), 6.47–6.41 (m, 4H, ArH), 2.11 (s, 6H, -CH₃) ppm. ¹³C NMR (150 MHz, CD₂Cl₂): δ 167.3, 166.4 (C=N), 147.7 (B-C_q), 143.7, 141.9, 137.2, 137.0 (C_q), 136.4 (C_q-CH₃), 135.4

(B-C_{Ar}), 133.6, 132.0 (C_{Ar,centralBenzene}), 131.7 (C_q-Cl), 130.9, 130.7, 130.3, 129.0, 128.7, 128.5, 128.2 (C_{Ar}), 127.5 (C_{Ar,centralBenzene}), 127.4, 126.6 (B-C_{Ar}), 21.2 (-CH₃) ppm. ¹¹B NMR (192 MHz, CD₂Cl₂): δ 2.6 (s, B_{quart} , $\nu_{1/2}$ ~ 600 Hz) ppm. HRMS (ESI): calcd for C₇₂H₅₇B₂Cl₂N₆ ([M + H]⁺) 1097.4224, observed 1097.4219. UV/VIS (dichloromethane): λ_{abs} (shape, $\tilde{\nu}$, ϵ) = 365 nm (p, 27 397 cm⁻¹, 19 000 L mol⁻¹ cm⁻¹), 297 nm (sh, 33 670 cm⁻¹, 22 800 L mol⁻¹ cm⁻¹). Fluorescence (dichloromethane): λ_{em} (shape, $\tilde{\nu}$) = 538 nm (p, 18 587 cm⁻¹), 469 nm (p, 21 322 cm⁻¹). Absolute quantum yield (dichloromethane): Φ_F = <1%. Absolute quantum yield (crystalline): Φ_F = 4%.

Synthesis of boron complex 14e. A flask under an inert atmosphere was charged with triphenylborane (460 mg, 1.86 mmol, 3.0 equiv.) and tris-triazapentadiene **6e** (690 mg, 0.63 mmol, 1.0 equiv.). After adding dry toluene, the reaction mixture was heated under refluxing conditions for 4 h. After that time, the solvent was removed under reduced pressure and the crude product was subjected to column chromatography on neutral alumina with 90% cyclohexane and 10% ethyl acetate (R_f = 0.26) to furnish the tris-triazapentadiene boron compound **14e** as a yellow solid in 77% (768 mg) yield: mp 191 °C. ¹H NMR (600 MHz, CD₂Cl₂): δ 7.44 (s, 3H, ArH_{centralBenzene}), 7.43–7.41 (m, 12H, B-ArH), 7.41–7.39 (m, 6H, ArH), 7.13–7.09 (m, 18H, B-ArH), 7.09–7.05 (m, 6H, ArH), 6.67–6.60 (m, 12H, ArH), 6.56–6.49 (m, 6H, ArH), 6.05 (d, J_{HH} = 8.0 Hz, 6H, ArH), 2.23 (s, 9H, -CH₃), 2.11 (s, 9H, -CH₃), 2.08 (s, 9H, -CH₃) ppm. ¹³C NMR (150 MHz, CD₂Cl₂): δ 166.9, 165.2 (C=N), 147.7 (B-C_q), 142.4, 141.4, 140.8 (C_q), 136.1 (C_{q,centralBenzene}), 135.9, 135.7 (C_q-CH₃), 135.4 (B-C_{Ar}), 134.5 (C_q-CH₃), 133.3 (C_{Ar,centralBenzene}), 130.8, 129.2, 128.7, 128.4, 128.2 (C_{Ar}), 127.0, 126.1 (B-C_{Ar}), 21.6, 21.1, 20.9 (-CH₃) ppm. ¹¹B NMR (192 MHz, CD₂Cl₂): δ -2.8 (s br, B_{quart} , $\nu_{1/2}$ ~ 3000 Hz) ppm. HRMS (ESI): calcd for C₁₁₁H₉₇B₃N₉ ([M + H]⁺) 1588.8151, observed 1588.8167. UV/VIS (dichloromethane): λ_{abs} (shape, $\tilde{\nu}$, ϵ) = 363 nm (p, 27 548 cm⁻¹, 26 700 L mol⁻¹ cm⁻¹), 298 nm (p, 33 557 cm⁻¹, 33 400 L mol⁻¹ cm⁻¹). Fluorescence (dichloromethane): λ_{em} (shape, $\tilde{\nu}$) = 517 nm (p, 19 342 cm⁻¹), 479 nm (sh, 20 877 cm⁻¹). Absolute quantum yield (dichloromethane): Φ_F = <1%. Absolute quantum yield (crystalline): Φ_F = 2%.

Conclusions

In summary, we have described the modular synthesis and full structural characterization including X-ray diffraction analysis of two novel mono-1,3,5-triazapentadiene-boron complexes **14a,b**, two hitherto unknown bis-1,3,5-triazapentadiene-boron complexes **14c,d** and the first tris-triazapentadiene boron complex **14e**. In order to evaluate their photophysical properties all compounds were investigated by absorption and emission spectroscopy in solution as well as in the solid state. The experimentally observed relatively similar absorption properties in solution of **14a,c,e** were interpreted on the basis of quantum chemical TD-DFT calculations as a result of only



limited electron delocalization involving the central benzene ring and the neighboring triazapentadiene boron systems due to the specific steric properties. The inspection of the relevant Kohn–Sham molecular orbitals indicates that the photochemistry of all these systems **14** is based on intramolecular charge transfer processes (ICT). In contrast, the emission properties of the three classes of compounds differ significantly with respect to emission maxima and Stokes shifts. Quite interestingly, whereas the fluorescence in solution of the compounds **14a–e** is not visible to the naked eye, bright red-shifted emission was seen for these compounds in the solid state and, qualitatively, in an acetonitrile–water suspension. Most likely, steric bulk hindering the rotation of the substituents of these compounds in the solid state is responsible for these emission properties.

Acknowledgements

Financial support from the Deutsche Forschungsgemeinschaft (IRTG 1143 Münster-Nagoya and SFB 858) is gratefully acknowledged. This work was partly supported by JSPS Core-to-Core Program, A. Advanced Research Networks (S.Y.).

References

- H. Ley and F. Müller, *Ber. Dtsch. Chem. Ges.*, 1907, **40**, 2950–2958.
- J. A. Elvidge and N. R. Barot, *Imidines and diamidides (1,3,5-Triazapentadienes) Patai, The chemistry of functional groups, Suppl. A. The chemistry of doubly bonded functional groups part 2*, Wiley, London, 1977, ch. 13.
- F. C. Cooper, M. W. Partridge and F. W. Short, *J. Chem. Soc.*, 1951, 391–404.
- N. Heße, R. Fröhlich, B. Wibbeling and E.-U. Würthwein, *Eur. J. Org. Chem.*, 2006, 3923–3937.
- N. Heße, R. Fröhlich, I. Humelnicu and E.-U. Würthwein, *Eur. J. Inorg. Chem.*, 2005, 2189–2197.
- (a) H. V. R. Dias, J. A. Flores, M. Pellei, B. Morresi, G. G. Lobbia, S. Singh, Y. Kobayashi, M. Yousufuddin and C. Santini, *Dalton Trans.*, 2011, **40**, 8569–8580; (b) M. N. Kopylovich and A. J. L. Pombeiro, *Coord. Chem. Rev.*, 2011, **255**, 339–355; (c) J. Barker and M. Kilner, *J. Chem. Soc., Dalton Trans.*, 1989, 837–841; (d) F. Liu, X. Qiao, M. Wang, M. Zhou, H. Tong, D. Gup and D. Liu, *Polyhedron*, 2013, **52**, 539–544; (e) A. Igashira-Kamiyama, T. Kajiwara, T. Konno and T. Ito, *Inorg. Chem.*, 2006, **45**, 6460–6466; (f) V. A. K. Adiraju, J. A. Flores, M. Yousufuddin and H. V. R. Dias, *Organometallics*, 2012, **31**, 7925–7932 and references therein; (g) N. Q. Shixaliyev, A. M. Maharramov, A. V. Gurbanov, V. G. Nenajdenko, V. M. Muzalevskiy, K. T. Mahmudov and M. N. Kopylovich, *Catal. Today*, 2013, **217**, 76–79. and references therein.
- (a) K. Bakthavachalam and N. D. Reddy, *Organometallics*, 2013, **32**, 3174–3184; (b) J. Masuda and D. W. Stephan, *Dalton Trans.*, 2006, 2089–2097.
- D. R. Aris, J. Barker, P. R. Phillips, N. W. Alcock and M. G. H. Wallbridge, *J. Chem. Soc., Dalton Trans.*, 1997, 909–910.
- H. V. R. Dias, S. Singh and T. R. Cundari, *Angew. Chem., Int. Ed.*, 2005, **44**, 4907–4910.
- (a) A. Treibs and F.-H. Kreuzer, *Liebigs Ann. Chem.*, 1968, **718**, 208–223; (b) A. Loudet and K. Burgess, *Chem. Rev.*, 2007, **107**, 4891–4932; (c) Q.-D. Liu, M. S. Mudadu, R. Thummel, Y. Tao and S. Wang, *Adv. Funct. Mater.*, 2005, **15**, 143–154; (d) J. A. Araneda, W. E. Piers, B. Heyne, M. Parvez and R. McDonald, *Angew. Chem., Int. Ed.*, 2011, **50**, 12214–12217.
- D. Frath, J. Massue, G. Ulrich and R. Ziesel, *Angew. Chem., Int. Ed.*, 2014, **53**, 2290–2310.
- (a) Y.-L. Rao and S. Wang, *Inorg. Chem.*, 2011, **50**, 12263–12274; (b) G. E. Morse and T. P. Bender, *ACS Appl. Mater. Interfaces*, 2012, **4**, 5055–5068; (c) Z. M. Hudson and S. Wang, *Dalton Trans.*, 2011, **40**, 7805–7816.
- J. R. Milks, G. W. Kennerly and J. H. Polevy, *J. Am. Chem. Soc.*, 1962, **84**, 2529–2534.
- (a) V. A. Dorokhov, B. M. Zolotarev, O. S. Chizhov and B. M. Mikhailov, *Izv. Akad. Nauk SSSR, Ser. Khim.*, 1977, **7**, 1587–1593; (b) B. M. Mikhailov, V. A. Dorokhov and V. I. Seredenko, *Izv. Akad. Nauk SSSR, Ser. Khim.*, 1977, **6**, 1385–1390; (c) B. M. Mikhailov, *Pure Appl. Chem.*, 1977, **49**, 749–764; (d) O. G. Boldyreva, V. A. Dorokhov and B. M. Mikhailov, *Izv. Akad. Nauk SSSR, Ser. Khim.*, 1985, **2**, 428–430.
- (a) K. B. Anderson, R. A. Franich, H. W. Kroese, R. Meder and C. E. F. Rickard, *Polyhedron*, 1995, **14**, 1149–1153; (b) G. Sathyamoorthi, M.-L. Soong, T. W. Ross and J. H. Boyer, *Heteroat. Chem.*, 1993, **4**, 603–608.
- I. Häger, R. Fröhlich and E.-U. Würthwein, *Eur. J. Org. Chem.*, 2009, 2415–2428.
- (a) M. A. Dureen and D. W. Stephan, *J. Am. Chem. Soc.*, 2010, **123**, 13559–13568; (b) D. Zhao, G. Li, D. Wu, X. Qin, P. Neuhaus, Y. Cheng, S. Yang, Z. Lu, X. Pu, C. Long and J. You, *Angew. Chem., Int. Ed.*, 2013, **52**, 13676–13680.
- (a) B. Neue, R. Fröhlich, B. Wibbeling, A. Fukazawa, A. Wakamiya, S. Yamaguchi and E.-U. Würthwein, *J. Org. Chem.*, 2012, **77**, 2176–2184; (b) B. Neue, A. Wakamiya, R. Fröhlich, B. Wibbeling, S. Yamaguchi and E.-U. Würthwein, *J. Org. Chem.*, 2013, **78**, 11747–11755.
- (a) D. Wang, R. Liu, C. Chen, S. Wang, J. Chang, C. Wu, H. Zhu and E. R. Waclawik, *Dyes Pigment.*, 2013, **99**, 240–249; (b) Y. Deng, Y.-y. Cheng, H. Liu, J. Mack, H. Lu and L.-g. Zhu, *Tetrahedron Lett.*, 2014, **55**, 3792–3796.
- J. I. Clodt, C. Wigbers, R. Reiermann, R. Fröhlich and E.-U. Würthwein, *Eur. J. Org. Chem.*, 2011, 3197–3209.
- C. Glotzbach, U. Kauscher, J. Voskuhl, N. S. Kehr, M. C. A. Stuart, R. Fröhlich, H. J. Galla, B. J. Ravoo, K. Nagura, S. Saito, S. Yamaguchi and E.-U. Würthwein, *J. Org. Chem.*, 2013, **78**, 4410–4418.
- J. Luo, Z. Xie, J. W. Y. Lam, L. Cheng, H. Chen, C. Qiu, H. S. Kwok, X. Zhan, Y. Liu, D. Zhu and B. Z. Tang, *Chem. Commun.*, 2001, **36**, 1740–1741.
- (a) C. Kitamura, Y. Tanigawa, T. Kobayashi, H. Naito, H. Kurata and T. Kawase, *Tetrahedron*, 2012, **68**, 1688–1694; (b) A. Dreuw, J. Plötner, L. Lorenz, J. Wachtveitl,



- J. E. Djanhan, J. Brüning, T. Metz, M. Bolte and M. U. Schmidt, *Angew. Chem., Int. Ed.*, 2005, **44**, 7783–7786; (c) H. Langhals, T. Potrawa, H. Nöth and G. Linti, *Angew. Chem., Int. Ed. Engl.*, 1989, **28**, 478–480.
- 24 (a) J. Chen, C. C. W. Law, J. W. Y. Lan, Y. Dong, S. M. F. Lo, I. D. Williams, D. Zhu and B. Z. Tang, *Chem. Mater.*, 2003, **15**, 1535–1546; (b) G. Yu, S. Yin, Y. Liu, J. Chen, X. Xu, X. Sun, D. Ma, X. Zhan, Q. Peng, Z. Shuai, B. Z. Tang, D. Zhu, W. Fang and Y. Luo, *J. Am. Chem. Soc.*, 2005, **127**, 6335–6346; (c) Y. Hong, J. W. Y. Lam and B. Z. Tang, *Chem. Commun.*, 2009, **44**, 4332–4353.
- 25 (a) A. D. Becke, *J. Chem. Phys.*, 1993, **98**, 5648–5652; (b) C. Lee, W. Yang and R. G. Parr, *Phys. Rev. B: Condens. Matter*, 1988, **37**, 785–789; (c) P. J. Stephens, F. J. Devlin, C. F. Chabalowski and M. J. Frisch, *J. Phys. Chem.*, 1994, **98**, 11623–11627.
- 26 M. J. Frisch, G. W. Trucks, H. B. Schlegel, G. E. Scuseria, M. A. Robb, J. R. Cheeseman, G. Scalmani, V. Barone, B. Mennucci, G. A. Petersson, H. Nakatsuji, M. Caricato, X. Li, H. P. Hratchian, A. F. Izmaylov, J. Bloino, G. Zheng, J. L. Sonnenberg, M. Hada, M. Ehara, K. Toyota, R. Fukuda, J. Hasegawa, M. Ishida, T. Nakajima, Y. Honda, O. Kitao, H. Nakai, T. Vreven, J. A. Montgomery Jr., J. E. Peralta, F. Ogliaro, M. Bearpark, J. J. Heyd, E. Brothers, K. N. Kudin, V. N. Staroverov, R. Kobayashi, J. Normand, K. Raghavachari, A. Rendell, J. C. Burant, S. S. Iyengar, J. Tomasi, M. Cossi, N. Rega, J. M. Millam, M. Klene, J. E. Knox, J. B. Cross, V. Bakken, C. Adamo, J. Jaramillo, R. Gomperts, R. E. Stratmann, O. Yazyev, A. J. Austin, R. Cammi, C. Pomelli, J. W. Ochterski, R. L. Martin, K. Morokuma, V. G. Zakrzewski, G. A. Voth, P. Salvador, J. J. Dannenberg, S. Dapprich, A. D. Daniels, Ö. Farkas, J. B. Foresman, J. V. Ortiz, J. Cioslowski and D. J. Fox, *Gaussian 09, Revision D.01*, Gaussian, Inc., Wallingford CT, 2009.
- 27 (a) R. Bauernschmitt and R. Ahlrichs, *Chem. Phys. Lett.*, 1996, **256**, 454–464; (b) R. E. Stratmann, G. E. Scuseria and M. J. Frisch, *J. Chem. Phys.*, 1998, **109**, 8218–8224.
- 28 D. Hellwinkel, F. Laemmerzahl and G. Hofmann, *Chem. Ber.*, 1983, **116**, 3375–3405.
- 29 G. Tarzia, P. Schiatti, D. Selva, D. Favara and S. Ceriani, *Eur. J. Med. Chem.*, 1976, **11**, 263–270.
- 30 H. Nakajima, M. Takahashi and Y. Kimura, *Macromol. Mater. Eng.*, 2010, **295**, 460–468.
- 31 M. V. Zatssepina, T. V. Artamonova and G. I. Koldobskii, *Russ. J. Org. Chem.*, 2008, **44**, 577–581.
- 32 R. Kupfer, M. Nagel, E.-U. Würthwein and R. Allmann, *Chem. Ber.*, 1985, **118**, 3089–3104.

